PHYSICAL REVIEW B **88**, 041407(R) (2013)

Probing the chiral nature of electromagnetic fields surrounding plasmonic nanostructures

Nina Meinzer, Euan Hendry, and William L. Barnes
School of Physics and Astronomy, University of Exeter, Exeter EX4 4QL, United Kingdom
(Received 18 January 2013; published 29 July 2013)

We investigate the chiral properties of near fields around plasmonic nanostructures and their relation to the electromagnetic chirality C. By combining chiral metal nanoparticles with achiral dye molecules and measuring the circular polarization dependence of the enhanced photoluminescence, we find a correlation between the dissymmetry of the luminescence enhancement and the calculated values of C. These effects are strong ($\sim 10^{-1}$), despite the weak circular dichroism of the particles ($\sim 10^{-5}$). We further show that C represents the chiral selectivity of the near-field coupling between an emitter and a nanoantenna.

DOI: 10.1103/PhysRevB.88.041407 PACS number(s): 42.25.Ja, 78.55.−m, 78.67.Pt, 81.05.Xj

Structural chirality, i.e., the handedness of an object that makes it incongruent with its mirror image, is a common property of many biologically relevant molecules, ranging from simple amino acids to complex helical DNA strands. This quality is often characterized by optical techniques that exploit the enantioselective interaction with circularly polarized light, e.g., by measuring circular dichroism (CD),[1,2] or by detecting molecular transitions in chiral molecules.[3,4]

Such studies of chiroptical effects require an understanding of the chirality—or helicity—of light, which is not as simple a concept as structural chirality: It is, more fundamentally, associated with angular momentum. However, determining the connection between helicity and angular momentum is not trivial,[5] not even for a plane electromagnetic wave, and it breaks down entirely for evanescent fields.[6] Nevertheless, it has been shown that the evanescent near fields around certain plasmonic nanostructures can undergo chiroptical interactions.[7–12] However, the chiral properties of these electromagnetic near fields are very different from circularly polarized light; indeed, the concept of polarization is not applicable to evanescent fields: They exhibit phase-shifted electric and magnetic field vector components without temporal vector rotation. Such solutions to the Maxwell equations are only allowed in local regions of space, such as in the vicinity of scattering nanostructures or at the center of Laguerre-Gaussian beams.[13]

A more general description of the chiral symmetry of arbitrary electromagnetic fields is therefore needed and several theoretical approaches have been proposed.[14–17] We follow Ref. 15, wherein Tang and Cohen introduced the *electromagnetic chirality* (elsewhere also referred to as the *Lipkin zilch*[14] or the *optical chirality density*[17]),

$$C = -\frac{\epsilon_0}{2}\omega\,\mathrm{Im}(\mathbf{E}^*\ \mathbf{B}), \tag{1}$$

a pseudoscalar that serves as a measure of the chiral nature of an electromagnetic field with $\mathbf{E}$ and $\mathbf{B}$ denoting complex electric and magnetic field vectors, respectively. The formalism developed in Ref. 15 is based on the interaction of a time-varying electromagnetic field with the electric and magnetic dipole moments that describe a chiral probe molecule. The electromagnetic chirality is then linked to the dissymmetry in the excitation rate of this probe for left- and right-handed systems. It contains only the chirality intrinsic to the electromagnetic field and is independent of the probe.

Chirality is usually quantified through far-field measurements, more specifically, of the CD. Such a measurement does not probe the near-field chirality C. Here, we directly probe the near field by looking at the luminescence enhancement of achiral emitters placed within the near field of plasmonic nanostructures. In light of recent theoretical work concerned with the electromagnetic chirality C around plasmonic nanostructures,[18,19] we are thus able to experimentally investigate in what way C represents the chiral properties of plasmonic near fields.

Typically, emitters such as dye molecules or nanocrystals are employed as near-field probes because it is straightforward to measure their luminescence, which is enhanced by the presence of plasmonic structures. This luminescence enhancement is directly linked to the enhanced local density of optical states (LDOS) associated with the enhanced near fields[13,20] and can therefore be used to, e.g., map the near-field distributions of plasmonic structures.[21] However, in our experiments we do not seek to map the local field intensities but rather to study how the interaction with a chiral nanostructure alters the polarization state of the enhanced luminescence in the far field.

To this end, we make use of the fact that not only the magnitude of the near-field enhancement is important for the luminescence enhancement but also the spectral position and the far-field polarization of the associated plasmon mode.[22] This can be understood as a consequence of the coupling between the dipolar emitters and the plasmon modes in a simple mode-coupling picture.[23,24] Under typical experimental conditions, where randomly oriented emitters rather than a single, well-defined dipole source are considered, the overall emission without the plasmonic structures does not have a preferred polarization. The polarization state of the coupled system is thus dominated by the plasmonic mode, which therefore determines the polarization state of the enhanced luminescence associated with this eigenmode.

For the case of chiral eigenmodes the situation is not quite as simple: The electromagnetic chirality associated with a metal nanostructure is due to the interaction of phase-shifted electric and magnetic field components in the near fields [see Eq. (1)], which in turn result from plasmon resonances associated with a linear polarization. Since the probe emitters will also couple to these linear modes, the enhanced emission will always have a substantial component of linear polarization, which can be described as a superposition of equal parts

of left-circularly polarized (LCP, $C > 0$) and right-circularly polarized (RCP, $C < 0$) light. The only meaningful observable in the chiral case is therefore the difference between left- and right-handed luminescence enhancement, which we can relate to a nonvanishing value of C of the fields around the nanostructure, provided the emitter does not add an element of enantioselectivity.

The plasmonic nanostructures we use for our experiments are pairs of silver nanorods which are laterally shifted along their long axis. This arrangement ensures that the magnetic field of one nanorod is parallel to the electric field of the second nanorod.[18] If the two rods are shifted by half their length, the maxima of electric field (at the ends) and magnetic field (in the center), which exhibit a natural phase shift of $\pi/2$, overlap and thus maximize the electromagnetic chirality of the structure [see Eq. (1)]. The direction of the shift determines the sign of C of the near fields around the nanoparticles. As we will show, these structures exhibit a high electromagnetic chirality [Fig. 3(c)], even though their far-field circular dichroism is only small ($\sim 10^{-5}$; see the Supplemental Material[25]).

We fabricate the structures by a standard electron-beam-lithography process on indium tin oxide (ITO)-covered glass substrates with a subsequent thermal evaporation of 30 nm of silver, followed by a lift-off procedure. The nanorod pairs are arranged in a square lattice with a lattice constant of 500 nm to form arrays with a footprint of 50 μm $\times$ 50 μm. We produce several arrays of nanorod pairs (the individual rods are approximately 160 nm long, 60 nm wide, 30 nm thick, and the two rods are separated by 70 nm) with increasing lateral shift, and of the corresponding enantiomers on the same substrate.

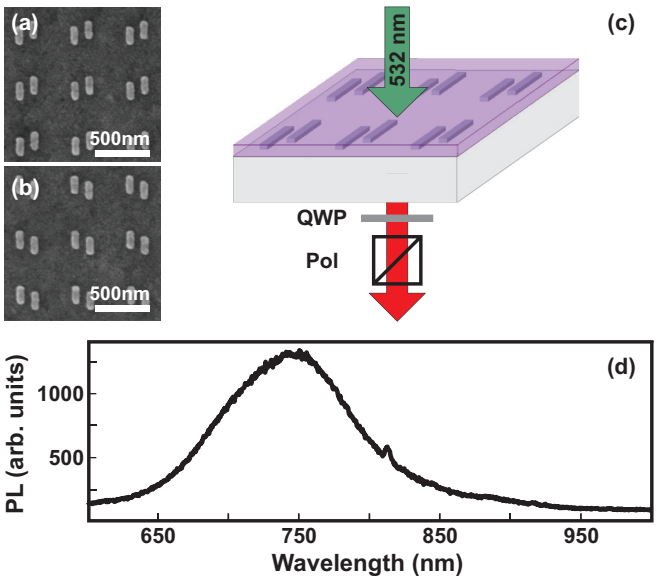

FIG. 1. (Color online) Scanning electron microscopy (SEM) micrographs of (a) left-handed and (b) right-handed silver nanorod pairs (approximately 160 nm long, 60 nm wide, 30 nm thick; separation 70 nm). (c) Schematic of our sample and of the measurements: The pump laser hits the sample from the polymer side and we analyze the luminescence on the substrate side with a quarter-wave plate (QWP) and a linear polarizer (Pol). (d) Photoluminescence spectrum of the dye-doped polymer film without metal structures.

As probe emitters we use achiral dye molecules (Styryl 9) doped into a 50-nm-thin polymer (polyvinyl alcohol) film with a dye molecule concentration of approximately 6.7×10^{19} cm^{-3}. This layer is prepared on top of the previously fabricated nanostructure arrays by spin coating. The dye-doped film has an emission maximum around 740 nm [Fig. 1(d)]. This way of applying the probe emitters breaks the sample symmetry perpendicular to the plane of the array and thus allows us to determine the electromagnetic chirality on this (polymer) side of the sample. If the nanostructures were symmetrically embedded in the dye-doped polymer, the overall effect would be zero.

We pump the dye molecules with a 532 nm cw laser at an average power of 15 μW impinging on the sample from the side of the polymer layer [Fig. 1(c)]. The laser is focused to a spot with a diameter of $\sim$30 μm. We detect the photoluminescence (PL) in the forward direction and analyze it with respect to its circular polarization states using a zero-order quarter-wave plate and a linear polarizer.

With the wave plate set to $+45^\circ$ and -45°, we measure the PL spectra on the nanorod-dimer arrays and we normalize them by dividing by the corresponding reference measurement on a nearby area of the dye-doped polymer film without nanostructures. By taking this ratio, we directly determine the PL enhancement factors f_{PL}^{+} and f_{PL}^{-} and can then calculate the dissymmetry between right- and left-handed enhancement as $\Delta f_{\mathrm{PL}} = f_{\mathrm{PL}}^{+} - f_{\mathrm{PL}}^{-}$, the difference between the two enhancement factors.

To minimize the influence of sample inhomogeneity, the measurements for all wave plate settings are taken at the same pump-spot position on an array and on the corresponding reference area, respectively. We also ensured that photobleaching of the dye molecules did not have a noticeable effect on our experimental data.

In our measurements we find the PL enhancement peak around 930 nm, corresponding to the spectral position of the plasmon resonance along the long axis of the nanorods (Fig. 2); this resonance in turn gives rise to the chiral eigenmode for laterally shifted arrangements of the two rods in a pair. This is in agreement with previously reported experiments on plasmonic PL enhancement.[22,26,27] However, our data also show a clear difference between the two enhancement factors f_{PL}^{+} (solid red line in Fig. 2) and f_{PL}^{-} (dashed blue line in Fig. 2) for chiral nanostructures.

In Fig. 3 we compare the dissymmetry in left- and right-handed PL enhancement $\Delta f_{\mathrm{PL}} = f_{\mathrm{PL}}^{+} - f_{\mathrm{PL}}^{-}$ measured on different structures: On an array of left-handed nanorod pairs [solid black curve in Fig. 3(a)] the PL enhancement for LCP is stronger than that for RCP, resulting in a positive value of Δf_{PL}. This dissymmetry is spectrally dependent, again in accordance with the plasmon resonance, with a maximum value of $\Delta f_{\mathrm{PL}} = 1$ corresponding to approximately 18% with respect to the maximum of f_{PL}^{+} (compare Fig. 2).

When we perform the same measurement on an array of the right-handed enantiomer [dashed green curve in Fig. 3(a)] we also find a distinct difference in the PL enhancement factors for LCP and RCP but with the right-handed PL now being more strongly enhanced, so that Δf_{PL} becomes negative. The spectral dependence of Δf_{PL} therefore roughly mirrors that of the left-handed structures with a minimum at the spectral

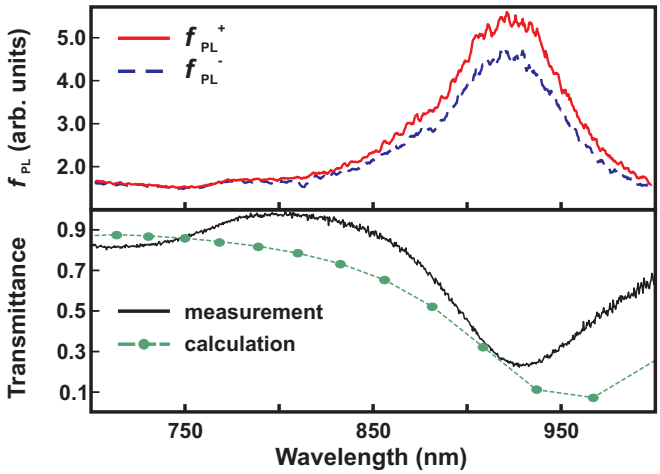

FIG. 2. (Color online) Photoluminescence enhancement spectra for left-handed nanorod pairs with the wave plate respectively set to ±45° and corresponding transmittance spectrum of the nanorod-pair array for linear polarization along the long axis of the rods. The solid black line shows the measured spectrum, and the green circles represent numerically modeled data.

position of the plasmon resonance and with a value of $\Delta f_{PL} = -1$ or -15% when normalized to the maximum of f_{PL}^{-}. For an achiral arrangement of the nanorod pair [Fig. 3(b)] we find no significant dissymmetry between left- and right-handed enhancement and Δf_{PL} is essentially zero for all wavelengths.

It is worth noting again that we find no difference in right- and left-handed emission on the dye-doped polymer film in the absence of the nanorods. The dissymmetry in PL enhancement we measure with the chiral nanostructures is thus evidence for the chiral properties of the plasmonic near fields.

To ensure that we measure effects due to the interaction of chiral near fields with the emitter molecules and not simply the circular dichroism of the structures when the PL generated in the dye-doped polymer layer passes through them, we performed a control experiment where we separated the nanorod-pair arrays from the polymer layer by an additional 200-nm-thick polymer [poly(methyl methacrylate) (PMMA)] spacer layer. This configuration does not allow the near fields, which have a decay length of several 10 nm, to interact with the dye molecules. For this control geometry we measure no difference in the PL signals for LCP and RCP, regardless of the chirality of the near fields around the structures on the polymer side.

Linear birefringence is another effect that could lead to similar results as the ones we measured. However, birefringence cannot occur if the biaxiality of the unit cell is broken. We therefore repeated our measurements on a second sample where the nanorod pairs are arranged in a fourfold (C_4) symmetric unit cell instead of a simple square lattice. For this sample layout we find the same dissymmetry in left- and right-handed PL enhancements as for the square lattice (see the Supplemental Material[25]) and therefore conclude that these effects do not arise from possible linear birefringence of the sample.

We have further repeated our measurements with the linear polarizer turned by 90°, so that the ±45° settings of the quarter-wave plate each correspond to the opposite handedness

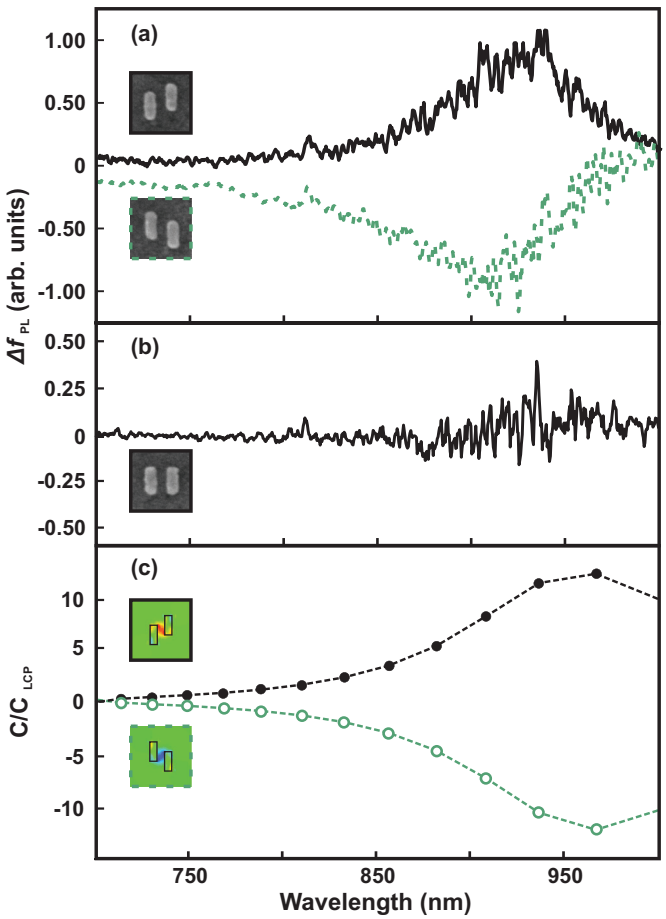

FIG. 3. (Color online) (a) Dissymmetry between left- and right-handed PL enhancement on two arrays of enantiomeric nanorod pairs. The dashed green line shows the data for the right-handed configuration, and the solid black line corresponds to the left-handed case. (b) The same for an achiral arrangement of equivalent nanorods. (c) Finite-element method (FEM) calculations of the normalized electromagnetic chirality C/C_{LCP} at the center of the unit cell in a plane 10 nm above the nanorod pairs for left-handed (solid black circles) and right-handed (open green circles) nanostructures. Dashed lines are added as a guide to the eye. The color scale for C/C_{LCP} in both insets ranges from −15 (blue) to +15 (red).

to that appropriate for the data shown above, in order to exclude any asymmetry in the wave plate. Again, we find the PL enhancement to be stronger for LCP light on left-handed nanorod pairs and for RCP light on right-handed structures with no difference for the achiral rod arrangement.

Overall, these experimental results agree well with the electromagnetic modeling of the chiral fields generated by the three different nanorod pairs [Fig. 3(c)]. We calculate the electromagnetic chirality C from the electric and magnetic fields determined by a full-wave finite-element model (ANSYS HFSS) at the center of the two-dimensional unit cell and 10 nm above the particles and normalize it by the electromagnetic chirality of LCP light, C_{LCP}. We model the nanostructures as rectangular blocks with 60 and 160 nm side lengths and a thickness of 30 nm; they are separated by a gap of 70 nm and for the chiral arrangements we assume a lateral shift of 80 nm. The rods are modeled as silver[28] on top of a glass

substrate ($n = 1.5$) and they are embedded in a medium with a refractive index 1.45. We use an adaptive mesh with an average element size of 5 nm in the vicinity of the nanostructures. The insets in Fig. 3(c) show the spatial distribution of C/C_{LCP} over one unit cell in a plane 10 nm above the particles for a left- and a right-handed arrangement, respectively. The calculations for a symmetric, i.e., achiral arrangement of the particles yield no hot spots of electromagnetic chirality (see the Supplemental Material[25]).

From Fig. 3(c) we see that the magnitude of the calculated electromagnetic chirality follows the same spectral trend as the PL enhancements in our experiments: For the right-handed case (open green circles) C/C_{LCP} becomes negative with a minimum around the resonance wavelength of the structure, while the left-handed case (solid black circles) mirrors this spectral trend and has positive values with a maximum at the resonance wavelength. Comparing these theoretical curves with our measured data in Fig. 3(a) clearly shows a correlation between the electromagnetic chirality C and the PL enhancements observed. We thus conclude that our measurements reflect the chiral properties of the near fields around our plasmonic nanostructures.

However, the question of how the chiral property of the near field described by C interacts with the emitter, and manifests itself in a preferential circular polarization in the far-field PL enhancement, remains unanswered at this point. Two mechanisms of how the chiral properties of the near fields are imprinted on the far field can be envisaged: Either the electromagnetic chirality can be interpreted as a chiral equivalent of the LDOS and will therefore cause the enhanced emission to have a preference for the handedness with a higher number of modes contributing to the chiral LDOS, or else the emitters excite the (chiral) eigenmodes of the plasmonic structures, which in turn control the far-field characteristics of the emitted light. In this picture, C describes the selective near-field coupling of the emitter to the nanoantenna, depending on the local chirality of the near field.

In order to clarify the nature of this interaction, we conduct a further experiment and repeat our measurements with the sample pumped from the substrate instead of the polymer side. This corresponds to observing the PL enhancement in the backward direction. In this excitation geometry, the dissymmetry in PL enhancement Δf_{PL} changes sign compared to the results shown in Fig. 3 (for details, see the Supplemental Material[25]). From this observation we conclude that the near-field interaction between emitters and nanoparticles results in the nanostructures acting as antennas with an emission pattern that directs LCP and RCP light in opposite directions, rather than altering the emission probabilities of the molecule for each handedness of circular polarization. The electromagnetic chirality C should thus be interpreted in the coupling picture, where it represents how the chirality of the near field dictates to which eigenmode of the nanoantenna the emitter preferentially couples.

By combining chiral nanostructures with achiral light-emitting molecules we can probe the electromagnetic chirality of the near field, even for a nanostructure whose far-field circular dichroism is relatively weak ($\sim 10^{-5}$). We have shown here that the near-field chirality is evident in a distinct dissymmetry for left- and right-handed PL enhancement for chiral nanorod pairs, depending on their handedness. We interpret the favored emission of a particular handedness as a manifestation of a chiral property of the plasmonic near fields, which is described by the electromagnetic chirality C. This explicitly demonstrates the chiral nature of the electromagnetic fields around the nanoparticles used for this work.

We thank Baptiste Auguie, Tim Davis, and Tom Philbin for helpful discussions. This work was supported through funding by The Leverhulme Trust and the EPSRC.

[1] *Circular Dichroism and Conformational Analysis of Biomolecules*, edited by G. D. Fasman (Plenum, New York, 1996).

[2] L. D. Barron, *Molecular Light Scattering and Optical Activity*, 2nd ed. (Cambridge University Press, Cambridge, UK, 2004).

[3] L. A. Nafie, *Vibrational Optical Activity: Principles and Applications* (Wiley, Hoboken, NJ, 2011).

[4] D. Patterson, M. Schnell, and J. M. Doyle, Nature (London) **497**, 475 (2013).

[5] S. M. Barnett, R. P. Cameron, and A. M. Yao, Phys. Rev. A **86**, 013845 (2012).

[6] K. Y. Bliokh and F. Nori, Phys. Rev. A **83**, 021803 (2011).

[7] J. K. Gansel, M. Thiel, M. S. Rill, M. Decker, K. Bade, V. Saile, G. von Freymann, S. Linden, and M. Wegener, Science **325**, 1513 (2009).

[8] M. Kuwata-Gonokami, N. Saito, Y. Ino, M. Kauranen, K. Jefimovs, T. Vallius, J. Turunen, and Y. Svirko, Phys. Rev. Lett. **95**, 227401 (2005).

[9] M. Decker, R. Zhao, C. M. Soukoulis, S. Linden, and M. Wegener, Opt. Lett. **35**, 1593 (2010).

[10] E. Hendry, T. Carpy, J. Johnston, M. Popland, R. V. Mikhaylovskiy, A. J. Lapthorn, S. M. Kelly, L. D. Barron, N. Gadegaard, and M. Kadodwala, Nat. Nanotechnol. **5**, 783 (2010).

[11] Y. Tang and A. E. Cohen, Science **332**, 333 (2011).

[12] V. K. Valev, J. J. Baumberg, C. Sibilia, and T. Verbiest, Adv. Mater. **25**, 2517 (2013).

[13] L. Novotny and B. Hecht, *Principles of Nano-Optics*, 2nd ed. (Cambridge University Press, Cambridge, UK, 2012).

[14] D. M. Lipkin, J. Math. Phys. (NY) **5**, 696 (1964).

[15] Y. Tang and A. E. Cohen, Phys. Rev. Lett. **104**, 163901 (2010).

[16] R. P. Cameron, S. M. Barnett, and A. M. Yao, New J. Phys. **14**, 053050 (2012).

[17] D. L. Andrews and M. M. Coles, Opt. Lett. **37**, 3009 (2012).

[18] E. Hendry, R. V. Mikhaylovskiy, L. D. Barron, M. Kadodwala, and T. J. Davis, Nano Lett. **12**, 3640 (2012).

[19] M. Schäferling, D. Dregely, M. Hentschel, and H. Giessen, Phys. Rev. X **2**, 031010 (2012).

[20]D. E. Chang, A. S. Sørensen, P. R. Hemmer, and M. D. Lukin, Phys. Rev. B. **76**, 035420 (2007).

[21]H. Ditlbacher, J. R. Krenn, N. Felidj, B. Lamprecht, G. Schider, M. Salerno, A. Leitner, and F. R. Aussenegg, Appl. Phys. Lett. **80**, 404 (2002).

[22]H. Mertens, J. S. Biteen, H. A. Atwater, and A. Polman, Nano Lett. **6**, 2622 (2006).

[23]H. Mertens, A. F. Koenderink, and A. Polman, Phys. Rev. B **76**, 115123 (2007).

[24]M. Wegener, J. L. García-Pomar, C. M. Soukoulis, N. Meinzer, M. Ruther, and S. Linden, Opt. Express **16**, 19785 (2008).

[25]See Supplemental Material at http://link.aps.org/supplemental/10.1103/PhysRevB.88.041407 for additional modelling and for experimental results of the control measurements discussed in the text.

[26]F. Tam, G. P. Goodrich, B. R. Johnson, and N. J. Halas, Nano Lett. **7**, 496 (2007).

[27]K. Tanaka, E. Plum, J. Y. Ou, T. Uchino, and N. I. Zheludev, Phys. Rev. Lett. **105**, 227403 (2010).

[28]*Handbook of Optical Constants of Solids*, edited by E. D. Palik (Academic, New York, 1985).